한국윤활학회지(1995), 제 11 권 제 5 호
*Journal of KSTLE(1995) Vol. 11, No. 5, pp.172~176*

# An Analysis on Surface Cracking Due to Thermomechanical Loading

S.S. Kim*, K.H. Lee** and S.M. Lee***

**Department of Mechanical Engineering, Kyung-pook National University, Daegu 702-701, Korea,*
***Department of Power Generation, Wolsung Nuclear Power Plant, 260, Naah-ri, Yangnam-myun, Kyungju-kun, Kyungpuk-do 788-840, Korea,*
****Department of Automobile, Ju-seong Junior College, Chungwon-kun, Chungpuk-do 363-930, Korea*

Abstract—This study deals with thermomechanical cracking between the friction surface and the interior of the brake disc. Analytical model considered in this study was a semi-infinite solid subjected to the thermal loading of an asperity moving with a high speed. The temperature field and the thermal stress state were obtained and discussed on the basis of Von Mises and Tresca Yielding Criterion. Analytical results showed that the dominant stress in cracking of friction brake is thermal stress and cracking location is dependent on the friction coefficient of contact and Peclet number. On the basis of analytical results thermomechanical cracking model is proposed.

**Key words** : Surface Cracking, Frictional Heating, Thermal Stress, Von Mises Yielding Criterion

## 1. Introduction

Friction brake disc is widely used to generate a retarding force by converting mechanical energy to thermal energy and to act as a storage and dissipation element for this thermal energy. When friction brake disc is in sliding contact under severe loading conditions, local high temperature may occur as a result of excessive frictional heating near the contacting surface. Because of a combination of thermal heating and the mechanical loading, numerous cracks are frequently found on the surfaces of brake disc. These cracks, called thermomechanical cracks or heat checks, contribute to excessive wear and fracture of the brake system.

Mow and Cheng [1] had analyzed theoretically the thermal stress on the elastic surface. Ju and his co-workers [2-4] a bearing seal, and Kennedy and Karpe [5] had analyzed thermocracking mechanism of a mechanical face seal by using finite element techniques. Recently, Limpert [6] investigated thermal conditions leading to surface rupture of cast iron rotors. This paper, considering the moving frictional heat source, deals with thermomechanical cracking at the frictional contact of brake disc. On the theoretical analysis a semi-infinite solid subjected to the thermal loading supplied externally with the Hertzian contact moving with a constant speed was considered.

## 2. Analytical Model

Fig. 1 shows the analytical model and the coordinate system for this analysis. The Hertzian pressure distribution is moving with constant velocity V on semi-infinite elastic surface. Here, the origin is the center of the Hertzian distribution with contact length 2c and the negative $y_1$ direction is downward. In Fig. 1, the pressure distribution $P(x_1)$ and the traction $T(x_1)$ are

$$P(x_1) = P_0\sqrt{1-(x_1/c)^2} \quad |x_1| \le c$$

$$T(x_1) = \mu P(x_1) \qquad y_1 = 0 \tag{1}$$

The frictional heat $Q(x_1)$ generated is given Eq. (2), and assumed the plane strain state.

$$Q(x_1) = \mu V P(x_1) \tag{2}$$

The dimensionless variables used for the theoretical analysis are defined as follows,

$$(x, y) = \left(\frac{x_1}{c}, \frac{y_1}{c}\right) \qquad P(x) = \frac{P(x_1)}{P_0}$$

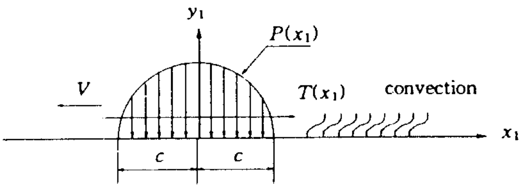


**Fig. 1. Analytical Model and Coordinate System.**

$$\phi=\frac{TK}{Qc} \qquad Pe=\frac{Vc}{k}$$

$$H=\frac{hc}{K}$$

$$h'=2G\frac{1+\nu}{1-\nu}\frac{\alpha k}{K} \qquad g=G\frac{1+\nu}{1-\nu}\frac{\alpha\mu}{K}Vc$$

## 2-1. Dimensionless Temperature Field

The heat equation for obtaining temperature field in Fig. 1 is

$$\frac{\partial^2 T}{\partial x_1^2}+\frac{\partial^2 T}{\partial y_1^2}=\frac{1}{k}\frac{DT}{Dt} \tag{3}$$

For quasistationary state, $\partial T/\partial t=0$ and $\partial x_1/\partial t=V$, $\partial y_1/\partial t=0$ : $DT/Dt=V\partial T/\partial x_1$. For high speed V, $\partial^2 T/\partial x_1^2$ may be neglected. Therefore, Eq. (3) becomes the following form

$$\frac{\partial^2 T}{\partial y_1^2}=\frac{V}{k}\frac{\partial T}{\partial x_1} \tag{4}$$

Since the frictional heat is imputed inside contact region and the heat loss by convection is happened outside, the boundary conditions of temperature fields are

$$K\frac{\partial T}{\partial y_1}=\begin{cases}-Q(x_1)\ (|x_1|\le c,\ y_1=0)\\ hT\quad (c<x_1<\infty,\ y_1=0)\end{cases}$$

$$T\to 0 \qquad [(x^2+y^2)^{\frac{1}{2}}\to\infty] \tag{5}$$

The dimensionless form of Eq. (4) and (5) are given as Eq. (6) and (7)

$$\frac{\partial^2\phi}{\partial y^2}=Pe\frac{\partial\phi}{\partial x} \tag{6}$$

$$\frac{\partial\phi}{\partial y}=\begin{cases}-P(x)\quad (|x|\le 1,\ y=0)\\ H\phi\ (1\le x\le\infty,\ y=0)\end{cases}$$

$$\phi\to 0 \qquad [(x^2+y^2)^{\frac{1}{2}}\to\infty] \tag{7}$$

Now, by Fourier transform and Laplace transform Eq. (6), (7) the dimensionless temperature field is given as Eq. (8) as the function of dimensionless coordinate (x,y) and Pe.

$$\phi(x,y)=\begin{cases}0 & (x<-1)\\ \frac{2}{\sqrt{\pi pe}}\int_{-1}^{x}P(t)(x-t)^{-\frac{1}{2}}e^{\frac{-Pey^2}{4(x-t)}}dt & (|x|\le 1)\\ \frac{2}{\sqrt{\pi Pe}}\int_{-1}^{1}P(t)(x-t)^{-\frac{1}{2}}e^{\frac{-pey^2}{4(x-t)}} & \\ \quad -H\int_{1}^{x}(x-t)^{-\frac{1}{2}}\phi(t,O)dt & (x>1)\end{cases} \tag{8}$$

## 2-2. Dimensionless Stress Field

### 2-2-1. Particular Stress Solution

For the solution of particular stress field under the contact surface, Duhamel-Neumann's stress -displacement equation is given as Eq. (9)

$$\sigma_{ij}=G(u_{i,j}+u_{j,i})+\lambda u_{k,k}\delta_{ij}-(3\lambda+2G)\alpha T\delta_{ij} \tag{9}$$

where G, $\lambda$ are Lame's constants, $u_{i,j}$ represents $u_i/x_j$.

After Eq. (9) is taken the dimensionless form, each stress components is represented as Eq. (10)

$$\sigma^p_{xx}=\frac{\sigma_{11}}{G}=2\frac{\partial u}{\partial x}+r\left(\frac{\partial u}{\partial x}+\frac{\partial v}{\partial y}\right)-(3r+2)\beta\phi$$

$$\sigma^p_{yy}=\frac{\sigma_{22}}{G}=2\frac{\partial v}{\partial y}+r\left(\frac{\partial u}{\partial x}+\frac{\partial v}{\partial y}\right)-(3r+2)\beta\phi$$

$$\sigma^p_{xy}=\frac{\sigma_{12}}{G}=\frac{\partial u}{\partial y}+\frac{\partial v}{\partial x} \tag{10}$$

where

$$\sigma^p_{xx}=\frac{\sigma_{11}}{G},\quad \sigma^p_{yy}=\frac{\sigma_{22}}{G},\quad \sigma^p_{xy}=\frac{\sigma_{12}}{G}$$

$$\beta=\frac{\alpha Qc}{K},\quad u=\frac{u_1}{c},\qquad v=\frac{v_1}{c}$$

$$r=\frac{\lambda}{G}$$

By using the temperature field Eq. (8), the impulse particular stress solution with unit pressure is obtained the following form

$$\delta\sigma^p_{xx}/P_o=\frac{1}{\sqrt{\pi Pe}}0.5fh'[Pey^2-2x-4Pex^2]$$

$$\times x^{-\frac{5}{2}}Exp(-Pey^2/4x)$$

$$\delta\sigma^{p}_{yy}/P_o = \frac{1}{\sqrt{\pi Pe}} 0.5fh'[2x-Pey^2]\, x^{-\frac{5}{2}} \times Exp(-Pey^2/4x)$$

$$\delta\sigma^{p}_{xy}/P_o = \frac{1}{\sqrt{\pi Pe}} 0.5fh'[2Peyx] \times^{-\frac{5}{2}} \times Exp(-Pey^2/4x) \quad (11)$$

### 2-2-2. Complementary Stress Solution

The complementary stress solution under the contact surface can be obtained from the harmonic function as Eq. (12).

$$\nabla^2\Omega = 0 \quad (12)$$

$\Omega$ is Airy's stress function and each complementary solution is represented by the secondary order of partial differential of $\Omega$.

$$\sigma^{c}_{xx} = \frac{\partial^2\Omega}{\partial y^2} \qquad \sigma^{c}_{yy} = \frac{\partial^2\Omega}{\partial x^2} \qquad \sigma^{c}_{xy} = -\frac{\partial^2\Omega}{\partial x\partial y} \quad (13)$$

In Fig. 1, the boundary conditions are given as Eq.(14) by the contact pressure and the frictional pressure from it.

$$\sigma_{yy} = \sigma^{p}_{yy} + \sigma^{c}_{yy} = P_o P(x)$$
$$\sigma_{xy} = \sigma^{p}_{xy} + \sigma^{c}_{xy} = \mu P_o P(x) \quad (14)$$

Complemently stress solution can be obtained as follows.

$$\delta\sigma^{c}_{xx}/P_o = (2\pi Pe)^{-\frac{1}{2}} fh'(x^2+y^2)^{-\frac{3}{4}} A_{yy} + 2[y+(2h'-1)fx]\, x^2(x^2+y^2)^{-2}/\pi$$
$$\delta\sigma^{c}_{yy}/P_o = (2\pi Pe)^{-\frac{1}{2}} fh'(x^2+y^2)^{-\frac{3}{4}} A_{xy} + 2[y+(2h'-1)fx]\, y^2(x^2+y^2)^{-2}/\pi$$
$$\delta\sigma^{c}_{xy}/P_o = (2\pi Pe)^{-\frac{1}{2}} fh'(x^2+y^2)^{-\frac{3}{4}} A_{xy} + 2[y+(2h'-1)fx]xy(x^2+y^2)^{-2}/\pi \quad (15)$$

where

$$A_{xx} = \cos\theta_1 + \sin\theta_1 - 1.5\cos\theta_o(\cos\theta_2 + \sin\theta_2)$$
$$A_{yy} = \cos\theta_1 + \sin\theta_1 + 1.5\cos\theta_o(\cos\theta_2 + \sin\theta_2)$$
$$A_{xy} = 1.5\cos\theta_o(\cos\theta_2 - \sin\theta_2)$$
$$\theta_o = \tan^{-1}(x-t/y)$$
$$\theta_1 = 1.5\theta_o \qquad \theta_2 = 2.5\theta_o$$

### 2-2-3. Stress Field

With the particular solution Eq. (10) and the complementary solution Eq. (15), the dimensionless stress field P(x) is given as Eq. (16)

$$\sigma^{o}_{ij}/P_o = \int_{-1}^{1} P(t)\delta\sigma^{c}_{ij}(x-t,y)dt - H\int_{1}^{\infty}\phi(t,0)\delta\sigma^{c}_{ij}(x-t,y)dt \qquad x \le -1$$

$$\sigma^{o}_{ij}/P_o = \int_{-1}^{x} P(t)\delta\sigma^{p}_{ij}(x-t,y)dt + \int_{-1}^{1} P(t)\delta\sigma^{c}_{ij}(x-t,y)dt - H\int_{1}^{\infty}\phi(t,0)\delta\sigma^{c}_{ij}(x-t,y)dt \qquad -1 < x \le 1$$

$$\sigma^{o}_{ij}/P_o = \int_{-1}^{1} P(t)\delta\sigma^{p}_{ij}(x-t,y)dt - H\int_{1}^{x}\phi(t,0)\delta\sigma^{p}_{ij}(x-t,y)dt + \int_{-1}^{1} p(t)\delta\sigma^{c}_{ij}(x-t,y)dt - H\int_{1}^{\infty}\phi(t,0)\delta\sigma^{c}_{ij}(x-t,y)dt \qquad x > 1 \quad (16)$$

## 3. Results and Discussion

Stress fields of Eq. (16) were obtained by using Romberg Integral Method. Typical friction test of commercial vehicle brake disc shows the friction coefficient value of 0.4. On the basis of this experimental result of brake test, we calculated the stress fields for $\mu$=0.4. For comparison, we computed them for $\mu$=0.1 and 0.7. These values of friction coefficient correspond to the boundary lubrication and unlubricated condition respectively. We also used three values of Peclet number to discuss the Peclet number's influence on the location of the maximum thermomechanical stress as well as the problem of frictional dependence. Recently cast iron is widely used in the friction brake system. By using the material properties of cast iron and actual vehicle's speed we computed the stress fields for Pe=3.83, 38.3, and 153.3. These values correspond to vehicle speed of 10 km/h, 100 km/h, and 400 km/h respectively. Kennedy and Karpe [5] showed the connection between the predicted plastic deformation in the contact and the incidence of thermo-cracking. It is known that if a localized region is deformed plastically in compression, but is surrounded by a large elastic region, and if the condition causing the plastic deformation is released, then residual stresses are set up in the deformed region which are tensile in nature [6]. If the amount of plastic deformation in the local

**Table 1. The maximum values of $\sqrt{J_2}/P_o$ and their positions**

| | Pe=3.83 | Pe=38.3 | Pe=153.3 |
|---|---|---|---|
| $\mu$=0.1 | 0.597<br>x=0.0 | 0.610<br>x=0.2 | 0.663<br>x=0.4 |
| $\mu$=0.4 | 1.058<br>x=0.05 | 1.307<br>x=0.7 | 1.852<br>x=1.0 |
| $\mu$=0.7 | 1.572<br>x=0.15 | 2.140<br>x=0.8 | 3.161<br>x=1.0 |

contact is very large, then the tensile residual stresses could be very large. Thus tensile cracks could be initiated. Plastic deformation can be predicted by the von Mises yield criterion, $\sqrt{J_2}$. We estimated the possibility of surface cracking on the basis of von Mises yield criterion. Fig. s 2 (a) and (b) $\sqrt{J_2}/P_o$ show distribution of von Mises Parameter $\sqrt{J_2}/P_o$ for Pe=3.83, $\mu$=0.1, Pe=3.83, $\mu$=0.4 and for Pe=3.83, $\mu$=0.7 respectively. As can be seen in Fig. (a) maximum value of $\sqrt{J_2}/P_o$ is approximately located at the surface of contact and at the center of contact width(x=0.0). Fig. 2 (b) represents the effect of friction coefficient of contact. The value of $\sqrt{J_2}/P_o$ for $\mu$=0.4 is much larger than that for $\mu$=0.1. And the maximum value of $\sqrt{J_2}/P_o$ for $\mu$=0.4 is located at the point of x=0.05. Fig. 2(a) and (b) show the effect of increasing the friction to 0.1 and 0.4. Figs. 3(a), (b) and (c) represent the results for Pe=153.3, $\mu$=0.1 and Pe=153.3, $\mu$=0.4 and for Pe=153.3, $\mu$=0.7. Fig. 3(a) shows that the maximum value of $\sqrt{J_2}/P_o$ is located at the surface and at the point of X=0.4. Comparing to the result of Pe=3.83, Fig. 2(a), this point is positioned at the right side. Fig. 3(b) represents that value of $\sqrt{J_2}/P_o$ is much higher and maximum value of that is located at the trailing edge (x=1.0). Figs. 3(a) and (b) show the effect of increasing the Peclet number to 3.83 and 153.3. From figures 2 and 3 it is found that the region of maximum yield parameter moves toward the trailing edge of contact surface in both cases as the friction is increased and Peclet number

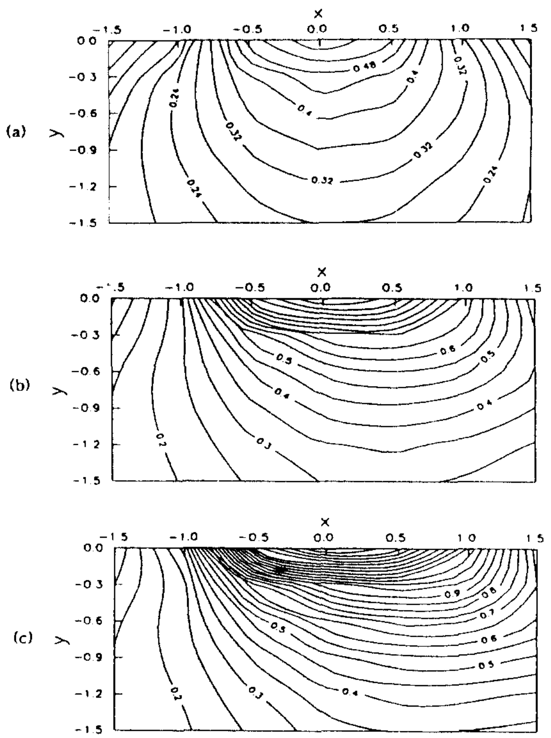

Fig. 2. Distribution of Von Mises parameter $\sqrt{J_2}/P_o$, (a) Pe = 3.83, $\mu$=0.1 (b) Pe = 3.38, $\mu$=0.4, (c) Pe=3.83, $\mu$=0.7.

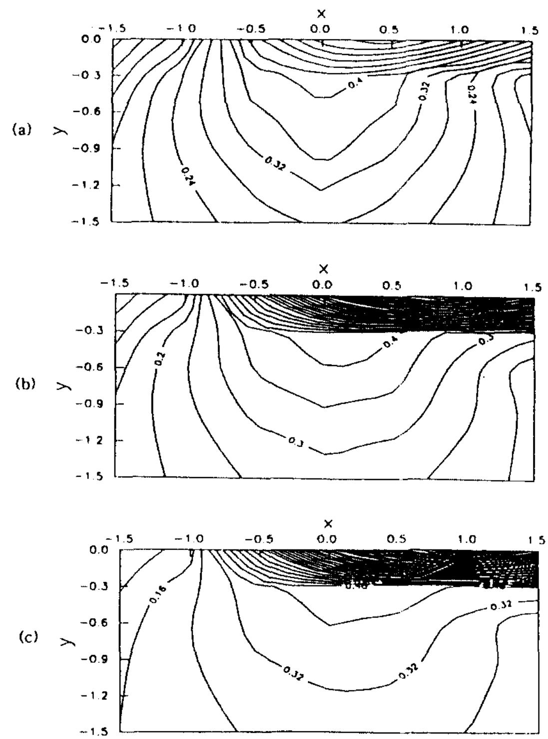

Fig. 3. Distribution of Von Mises parameter $\sqrt{J_2}/P_o$, (a) Pe=153.3, $\mu$=0.1 (b) Pe=153.3, $\mu$=0.4 (c) Pe=153.3, $\mu$=0.4.

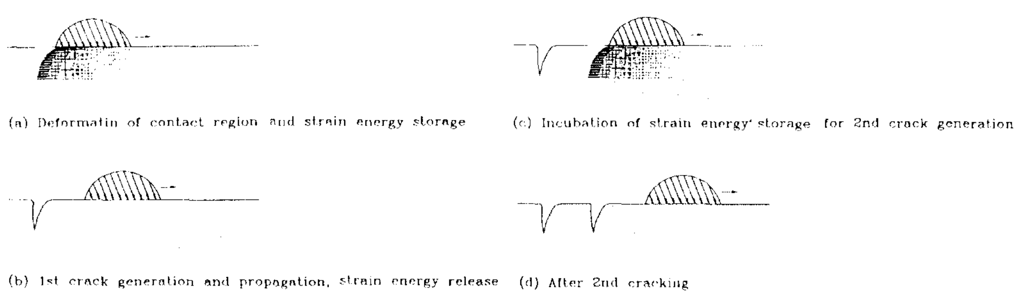


**Fig. 4. Schematic representation of multiple surface cracks.**

increase. We also computed the von Mises Parameter for Pe=38.3. It is summarized in Table 1.

If a surface crack is initiated in the region of residual stress, it would tend to relieve the residual strain energy, lowering the residual stress around it. Thus, a contact region would have to move a good distance away from a surface crack before building up a residual stress level sufficient to cause another crack to generate. Fig. 4 shows schematic representation of surface cracking procedure due to ther momechamical loading.

As contact region moves to the right, it is deformed and the strain energy of material under the contact region is stored. When the total strain energy becomes equal to or exceeds the critical strain energy corresponding to failure stress of the material, a crack forms and grows. As the crack is growing the strain energy stored under the contact region will be released and the growth of the crack will stop. The incubation period of strain energy accumulation for other crack generatiion will be required.

## 4. Conclusion

It has been analyzed that thermomechanical cracking in a friction brake disc modeled as a semi-infinite solid subjected to the thermomechanical loading of an asperity moving with a high speed. It was found that thermomechanical cracking location moves toward the trailing edge of contact surface and becomes more intense as friction and Peclet number increase. Friction and Peclet number are to dominate the thermomechanical cracking of friction brake disc. Ther momechanical surface cracking model was proposed.

## Acknowledgment

This reseach was partially supported by the Korea Reserch Foundation under Grant No. 01-E-0025, 1994.

## Symbols Used

G = elastic modulus(Pa)
K = thermal conductivity(W/mK)
Pe = Peclet number(Vc/k)
$P_o$ = maximum contact pressure
g = G(1+$\nu$) $\alpha$ f V c/(1-$\nu$)k
h = thermal convectivity
k = thermal diffusivity($m^2$/s)
$\alpha$ = linear expansion coefficient($K^{-1}$)
$\mu$ = frictional coefficient.
$\nu$ = Poisson's ratio
$\phi$ = dimensionless temperature field

## References

1. Mow, V.C. and Cheng, H.S., "Thermal Stress in an Elastic Half-space," ZAMP, Vol.18, pp. 500-507, 1967.
2. Ju, F.D. and John H. Huang, "Heat Checking in the Contact Zone of a Bearng Seal," Wear, Vol.79, pp. 107-118, 1982.
3. Ju, F.D. and Huang, J.H., "Thermo-mechanical Cracking due to Moving Frictional Loads," Wear, Vol.102, pp. 81-104, 1985.
4. Ju, F.D. and Liu, J.C., "Effect of Pecklet Number in Thermo-mechanical Cracking due to High Speed Friction Load," ASME, Journal of Tribology, Vol.110, pp. 217-221, 1988.
5. Kennedy, F.E. and Karpe, S.A., "Thermocracking of a Mechanical Face Seal," Wear, Vol.79, pp. 21-36, 1982.
6. Limpert, R., "An Investigation of Thermal Conditions Leading to Surface Rupture of Cast Iron Rotors," SAE, 720447, pp. 1507-1520, 1972.